BAYESIAN HYPOTHESIS TESTING: INTEGRATING FAST WELL-LOG FORWARD MODELING TO VALIDATE PETROPHYSICAL ROCK TYPING AND TO QUANTIFY UNCERTAINTY IN DEEPWATER RESERVOIRS

Chicheng Xu, Qinshan Yang, and Carlos Torres-Verdín
The University of Texas at Austin

This paper was prepared for presentation at the SPWLA 54th Annual logging Symposium held in New Orleans, Louisiana, June 22-26, 2013.

ABSTRACT

Rock typing is critical in deepwater reservoir characterization to construct stratigraphic models populated with static and dynamic petrophysical properties. However, rock typing based on multiple well logs is challenging because different logging-tool physics exhibit different volumes of investigation. Consequently, large uncertainty is typically associated with rock typing in thinly bedded or laminated reservoirs because true physical properties cannot be resolved due to shoulder-bed effects. To circumvent this problem, we introduce a new Bayesian approach that inherently adopts the scientific method of iterative hypothesis testing to perform rock typing by simultaneously honoring different logging-tool physics in a multi-layered earth model. In addition to estimating the vertical distribution of rock types with maximum likelihood, the Bayesian method quantifies the uncertainty of rock types and associated petrophysical properties layer-by-layer.

Bayesian rock classification is performed with a fast sampling technique based on the Markov-Chain Monte Carlo method, thereby enabling an efficient search of rock types to obtain final results. We use a fast linear iterative refinement method to simulate nuclear logs and a 2D forward modeling code to simulate array-induction resistivity logs. A rock-type distribution hypothesis is considered acceptable only when all observed well logs are reproduced with forward modeling.

Both synthetic and field cases are used to verify the effectiveness of the new rock typing method. In a field case of deltaic gas reservoirs from offshore Trinidad, the Bayesian method differentiates rock types that exhibit subtle petrophysical variations due to grain size change. We show that the new method provides more than 77% agreement between log-derived and core-derived rock types while conventional deterministic methods only achieve 60% agreement due to presence of thin beds and laminations. Rock types are verified with independent data sources such as laser particle size measurements and mercury injection capillary pressure.

Even though large uncertainty is observed in thinly bedded and laminated zones, the Bayesian rock-typing method still yields rock types and petrophysical properties that agree well with core-plug measurements acquired in these layers. As a result, the overall correlation between log-derived permeability and core-measured permeability is improved by approximately 16% when compared to conventional deterministic methods. More importantly, the quantified petrophysical uncertainty provides critical information for estimating the uncertainty of reservoir storage and productivity to guide decision-making for later phases of reservoir development.

INTRODUCTION

Conventional petrophysical rock typing heavily relies on representative laboratory core measurements, including mineral concentrations, grain-size and pore-size distribution, fluid saturation, and fluid distribution (Archie, 1950 and 1952; Buckles, 1965; Pittman, 1992). Significant effort has been placed on deriving rock types from well logs with minimum core calibration or supervision (Xu and Torres-Verdín, 2012a; Xu et al, 2012a; Xu and Torres-Verdín, 2013a). A common issue faced in log-based rock typing is that log-derived rock types do not match core-derived rock types to a satisfactory level in thinly bedded or laminated reservoirs. Furthermore, when rock typing is based on well logs, which are physical measurements indirectly sensing geological or petrophysical attributes, large uncertainty is commonly associated with rock typing due to overlapping of log responses for even the same geological or petrophysical rock type.

Forward physical modeling can predict unique well-log responses given a vertical distribution of rock types and their associated petrophysical properties. However, petrophysical interpretation, which aims to estimate rock petrophysical properties from well logs, is often subject to non-uniqueness, i.e., the concern of multiple working hypotheses in geosciences. This is particularly true when petrophysical thin beds are present. Unfortunately, such a simple fact has been routinely ignored in existing, deterministic apparent-log-based rock typing methods which generate only definite rock type distributions based on the philosophy of "*what I see is what I have.*" Therefore, such deterministic methods often fail to deliver accurate rock type distributions and lack the ability to quantify the uncertainty of rock types and their associated petrophysical properties.

In this paper, we approach rock typing by integrating a-priori core measurements and fast well-log forward modeling to test hypothetical rock type distributions based on quantitative comparisons between well logs and their numerical simulations. Efficient Bayesian sampling techniques (Yang and Torres-Verdín, 2011) are employed to narrow down the space of possible rock types in each petrophysical layer. The new method is capable of assimilating a-priori rock type information from core measurements. Furthermore, the bottom-up approach of building a hypothetical earth model allows closing the gap between log-scale and core-scale measurements. Uncertainty of rock types and petrophysical properties are also obtained after accumulating sufficient realizations of rock type distributions. The new method becomes a good example of integration of multiple disciplines, including numerical modeling, logging-tool physics and petrophysics, together with an explicit connection to a geological framework for enhanced reservoir description.

In the following sections, we first introduce the method and workflow of Bayesian rock typing, followed by a simple synthetic case that aims to illustrate the procedure of Bayesian rock typing. A field case of Deltaic gas reservoir from offshore Trinidad is then used to verify the performance of Bayesian rock typing in reservoir description.

METHOD AND WORKFLOW

Figure 1 shows the petrophysical workflow of log-based Bayesian rock typing. It begins with a hypothetical rock type distribution or earth model. Each rock type is associated with Gaussian distributions of various petrophysical properties. Well logs are then simulated numerically based on petrophysical properties at reservoir conditions. Available well logs are next compared to the numerically simulated logs to reject or accept the hypothetical rock type distribution. This procedure is iterated until a sufficient number of rock type realizations are obtained for further statistical analysis.

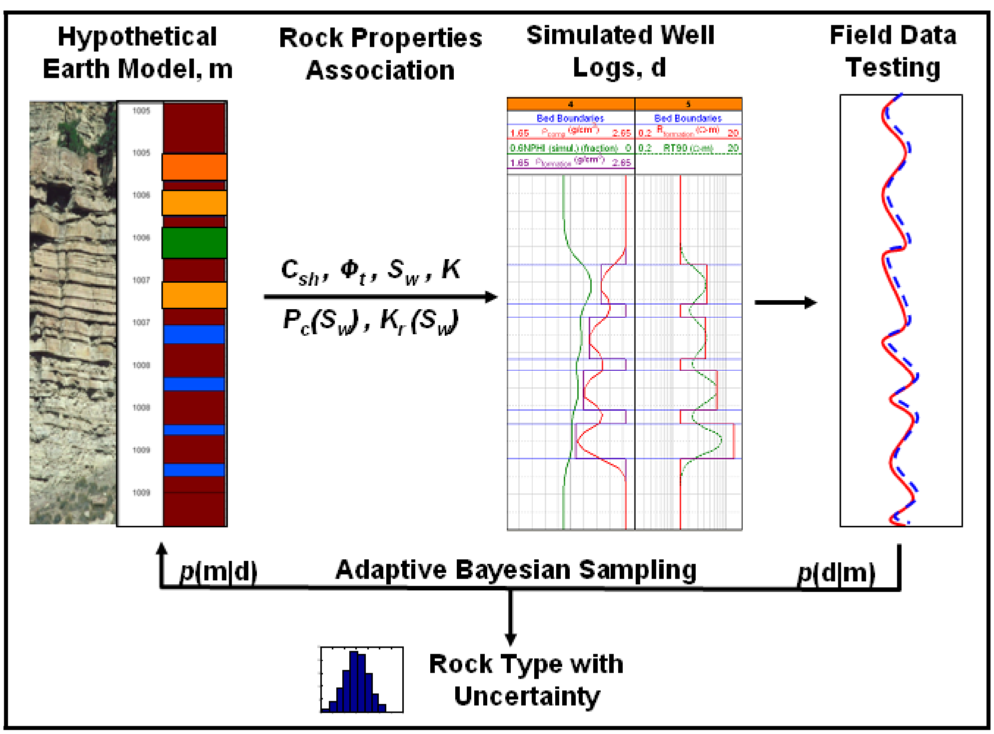

Fig. 1: Petrophysical workflow of well-log based Bayesian rock typing.

Fast Numerical Log Simulation in a Common Stratigraphic Framework. A multi-layered earth model, referred to as common stratigraphic framework (CSF) (Voss et al., 2009), is used to simulate well logs. We use a fast linear iterative refinement method to simulate nuclear logs (Mendoza et al., 2010; Ijasan, 2010) and a 2D forward modeling code to simulate array-induction resistivity logs (Wang et al., 2009).

The relationship between the earth model (**m**) and well logs (**d**) is referred to as the forward problem, given by

$$\mathbf{G}(\mathbf{m}) = \mathbf{d}, \qquad (1)$$

where **G** is the forward function, **m** is a vector of rock type distribution, and $\mathbf{d} = [\sigma_t, \rho_b, \phi_N, \gamma]^T$ is the vector of observed well logs based on the rock type distribution and their petrophysical properties. In this study, volumetric concentration, water saturation, total porosity, apparent electrical conductivity, bulk density, neutron porosity, and gamma ray are denoted by C_i, S_w, ϕ, σ_t, ρ_b, ϕ_N, and γ, respectively. To perform rock typing and quantify uncertainty, one needs to estimate vector **m** from the available well logs.

Statistical Description of Basis Rock Types. Rock type defines a set of rock samples that exhibit similar geological attributes, and/or petrophysical properties, and/or physical log responses. Therefore a rock type normally represents distributions of these properties instead of single-value properties. In our work, Gaussian (or log-normal) distributions are employed to describe rock properties. A statistical partitioning method is used to separate different rock types that exhibit significant overlapping rock properties (Vrubel, 2007; John et al., 2008). Figure 2 shows an example of the distributions of gamma ray values for four different rock types in a field case. We suggest that the statistical description of each rock property be obtained from thorough core study and used as a-priori information for Bayesian rock typing.

Bayesian Sampling of Rock Types. The Bayesian inversion process is essentially a stochastic search of earth models for which the simulated measurements agree with observations to a certain level. For an earth model of L layers and 5 rock types, there are 5^L hypothetical vertical rock type distributions to be tested during inference. We adopt an efficient and adaptive sampling technique to infer the most likely rock type distributions that honor the available well logs (Yang and Torres-Verdín, 2011).

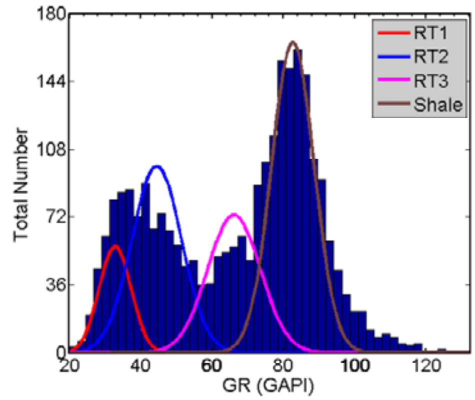

Fig. 2: Example of statistical distribution of gamma-ray values for four different rock types in a field case. Significant overlapping is observed between neighboring rock types.

Bayesian rock classification is performed with a fast sampling technique based on the Markov-Chain Monte Carlo method to enable efficient search of rock types. The idea of Markov-Chain Monte Carlo method is to generate random samples from the rock type posterior distribution by constructing a Markov chain. Yang and Torres-Verdín (2013) introduced an adaptive solution to generate the Markov chain. The solution is a set of rock types along the well trajectory which define the posterior distribution.

In this paper, we consider four well logs: density, neutron, resistivity, and gamma ray. We denote the a-priori distribution of formation properties by $p(\mathbf{m})$, the likelihood function by $p(\mathbf{d}|\mathbf{m})$, and the posterior probability distribution for properties by $q(\mathbf{m}|\mathbf{d})$. The prior distribution of properties is determined from prior field knowledge or other external information about the properties, such as core data. Tables 1 and 2 show examples of a-priori distributions of formation properties used in synthetic and field examples, respectively. The likelihood function measures the probability of observing the well logs, **d**, when the rock type distribution is **m**. On the other hand, the posterior distribution quantifies how well a rock type distribution agrees with prior information and available measurements.

Bayes' theorem relates a-priori and posterior distributions in a way that makes the computations of $q(\mathbf{m}|\mathbf{d})$ tractable (Aster et al., 2005). It can be written as

$$q(\mathbf{m} \mid \mathbf{d}) \propto p(\mathbf{d} \mid \mathbf{m})\, p(\mathbf{m}). \qquad (2)$$

Iterative Hypothesis Testing Against Well Logs. Once a vertical rock type distribution with associated petrophysical properties is sampled and populated into the predefined CSF, numerically simulated well logs are compared to field logs to test the hypothesis. A hypothesis of rock type distribution is only acceptable when all available well logs are reproduced with fast well log forward modeling given the hypothetical rock type distribution.

Yang and Torres-Verdín (2011) introduced a method to determine the number of steps needed to converge to the stationary distribution within an acceptable error. The procedure comes to a halt if any of the following two convergence criteria are met in the iteration process:

(1) The actual iteration number reaches the maximal iteration number, I_{max}, and,
(2) The accepted sample sequence is tested by a modified z-test and results reach the Geweke z-score requirement (Geweke, 1991).

Probabilistic Interpretation of Hybrid Rock Classes. Petrophysical zones segmented by well logs normally have a thickness ranging from 1 ft to 5 ft. In heterogeneous reservoirs, those intervals typically include hybrid rock classes composed of different basis rock types defined at the core scale. Two different approaches are used to describe hybrid rock classes: volumetric basis (Xu and Torres-Verdín, 2013b) and probabilistic basis. Figure 3 describes hybrid rock classes based on the probability of occurrence of each basis rock type.

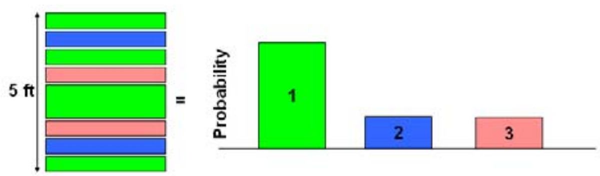

Fig. 3: Description of hybrid rock classes using a probabilistic approach. Rock type 1 exhibits the maximum likelihood in this example.

Uncertainty Quantification. After a certain number of hypothetic rock type distributions have been accepted after testing, the uncertainty of rock types in each layer can be analyzed in a statistical manner. A distribution of possible rock types in each layer can be visualized with a histogram which describes the rock type with the maximum likelihood and the associated standard deviation. The uncertainty of a given rock type thence propagates to the estimation of uncertainty of permeability, for instance.

Rock Type Validation. Contingency tables (Bishop et al., 1975) are used to quantify the agreement between core-derived and log-derived rock types in this paper. In a contingency table, the contingency coefficient, C, is defined as the ratio of diagonal elements to the total number of samples, and quantifies rock typing accuracy as

$$C = \sqrt{\frac{\chi^2}{N + \chi^2}}\ , \tag{3}$$

whereas Cramer's V quantifies the strength of the dependence between two variables as

$$V = \sqrt{\frac{\chi^2}{N(k-1)}}\ , \tag{4}$$

where N is the total number of rock samples, χ^2 is the Pearson's chi-squared test, and k is the number of rock types under comparison.

SYNTHETIC CASE: INTERBEDDED SAND-SHALE SEQUENCE

We construct a synthetic earth model of interbedded sand-shale sequences to illustrate the standard workflow of Bayesian rock typing. Five different rock types are assumed to be present in the reservoir: sands A, B, C, shaly sand D (with dispersed clay), and pure shale (SH). Sands A, B, and C were deposited with different flow energy; therefore they exhibit different grain sizes and reservoir quality. Shaly sand D has poor reservoir quality due to cementation of dispersed clay. Pure shales are non-reservoir facies. Table 1 lists the statistical descriptions of properties for each rock type.

Table 1: Statistical distributions of clay volume concentration, porosity, water saturation, and permeability for synthetic rock types.

	C_{cl} (frac)	ϕ_t (frac)	S_w (frac)
A	0.02 ± 0.01	0.25 ± 0.03	0.15 ± 0.05
B	0.02 ± 0.01	0.22 ± 0.04	0.25 ± 0.08
C	0.02 ± 0.01	0.20 ± 0.04	0.35 ± 0.10
D	0.05 ± 0.02	0.15 ± 0.04	0.55 ± 0.15
SH	1.0	0.12 ± 0.01	1.0

Figure 4 shows the synthetic earth model and the corresponding well logs (contaminated with 10%, zero-mean additive Gaussian noise), which are here regarded as field measurements. Uncertainty mainly originates from measurement noise and shoulder-bed effects. To test the Bayesian rock typing method, we assume that the earth model is unknown and use well logs to test various hypothetical rock type distributions and quantify how closely available well logs agree with their numerical simulations. The method starts with a prior earth model of all shales.

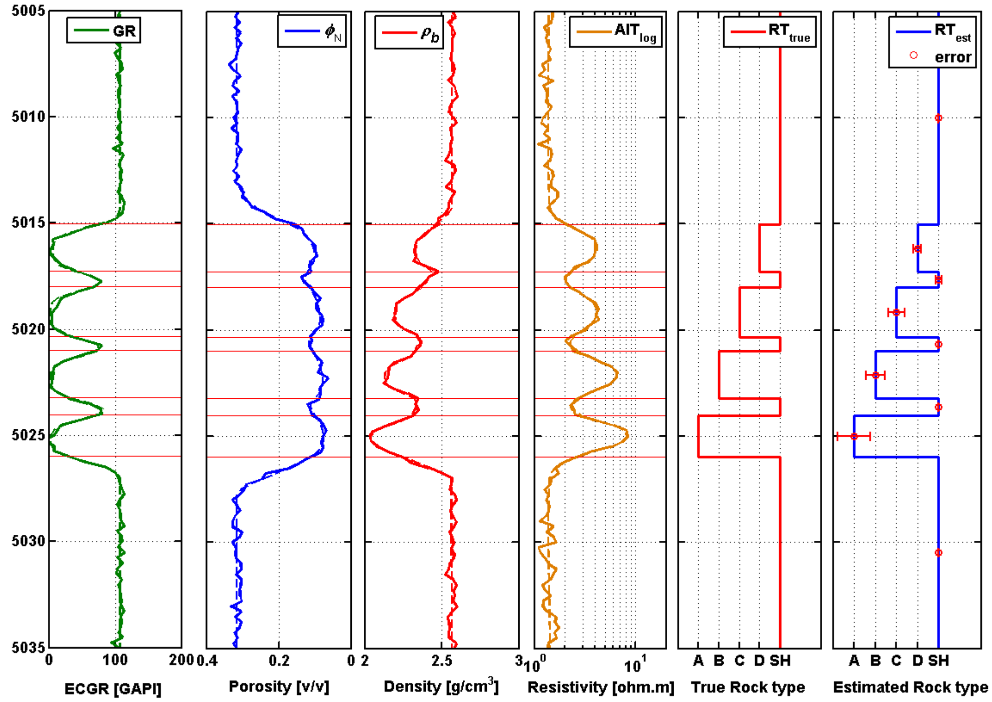

Fig. 4: Bayesian rock typing in a synthetic interbedded sand-shale sequence based on the corresponding simulated well logs. Solid lines: well logs with 10% additive, zero-mean Gaussian noise considered as field measurements in this synthetic case; Dashed lines: reproduced logs based on the rock type distribution with maximum likelihood.

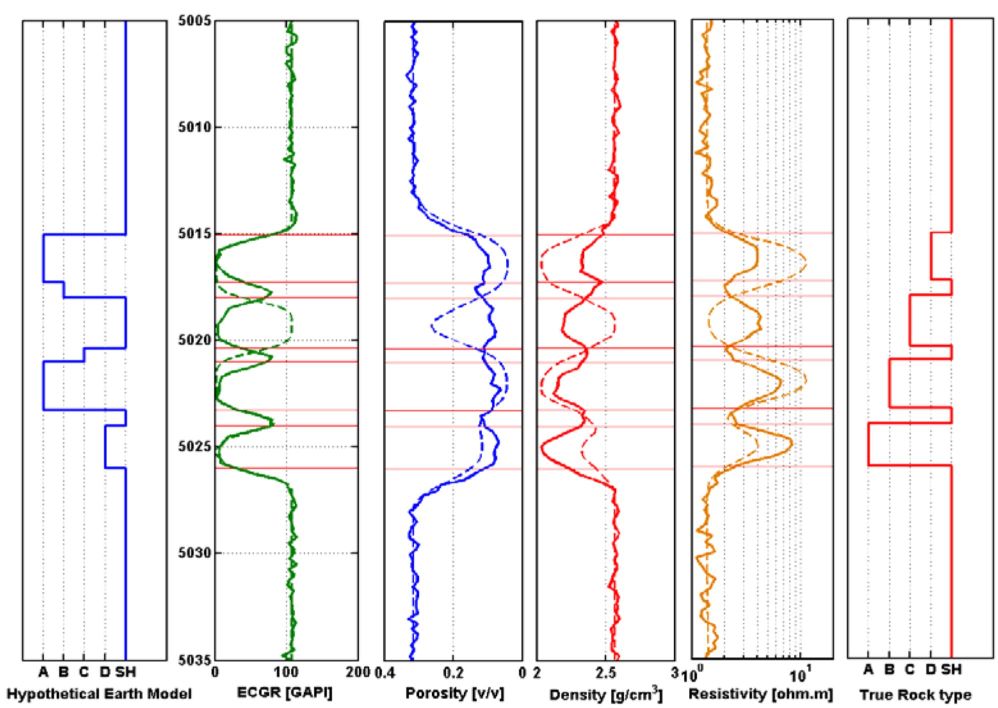

Fig. 5: Example of a rejected hypothetical rock type distribution. Simulated well logs significantly differ from those of the actual model.

Tracks 5 and 6 in Fig. 4 compare the synthetic earth model and the inferred earth model to results obtained with the Bayesian rock typing method. For each layer, the rock type with maximum likelihood agrees with the synthetic model, where the corresponding uncertainty is narrowly distributed in thick beds. This synthetic example confirms that the Bayesian method is capable of both inferring rock type distributions accurately and quantifying the uncertainty of a given rock type in each layer.

Figure 5 shows a hypothetical rock type distribution which significantly differs from the true earth model. Consequently, numerically simulated well logs also significantly differ from field measurements. This hypothetic rock type distribution should be rejected during the iterations leading to final estimation results. Such a procedure is in principle equivalent to the scientific method of iterative hypothesis testing.

Figure 6 shows the probabilistic descriptions of two shale layers. The thin bed exhibits relatively larger uncertainty than the thick bed due to shoulder-beds effects on well logs.

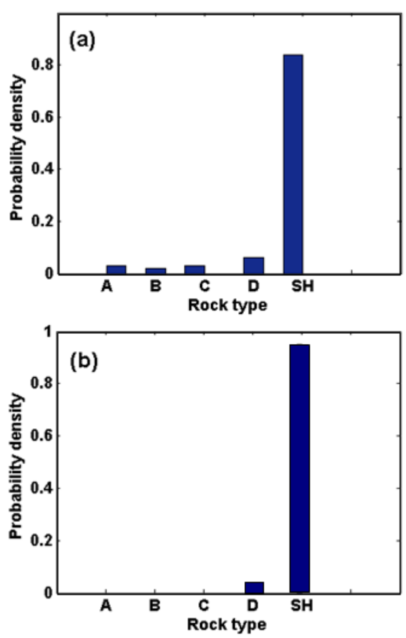

Fig. 6: Rock type uncertainty quantified in two petrophysical zones of the synthetic case. (a) Thin bed at 5018 ft, and (b) thick bed at 5010 ft.

FIELD CASE: DELTAIC GAS RESERVOIR, OFFSHORE TRINIDAD

The formation under consideration is a sandstone unit deposited in a deltaic sedimentary system in the Columbus Basin, offshore Trinidad (Liu, 2007; Xu and Torres-Verdín, 2012b). Different facies exhibit distinct grain-size distributions and clay volumetric concentrations, which result in different pore-size distributions (Xu and Torres-Verdín, 2013a). Therefore, a cause-effect relationship exists between depositional facies and hydraulic rock types. The reservoir is saturated with gas and was penetrated with a vertical key-study well drilled with synthetic oil-base mud (SOBM). Approximately 80 ft of whole core were acquired in the upper deltaic sequence for both geological and petrophysical studies. The cored zone was estimated to be at a height above free water level (HAFWL) between 400 and 500 ft. High in-situ capillary pressure between gas and water phases ensures that water saturation be close to irreducible saturation. Fluorescence analysis on sliced whole core confirmed that the invasion of SOBM during coring was negligible. Helium porosity, gas permeability (with Klinkenberg effect correction), and Dean-Stark water saturation were measured on 104 preserved core plugs, among which 11 core plugs were further subject to mercury injection capillary pressure (MICP) measurement and 24 core plugs were studied with a laser particle size analyzer (LPSA). The effects of mud-filtrate invasion on well logs are negligible due to very shallow radial length of invasion and absence of free water.

Basis Rock Classes from Core Measurements. We performed rock typing with Leverett's reservoir quality index (1941) calculated from routine porosity-permeability data (Fig. 7a) and studied the core-measured water saturation of each rock type (Fig. 7b). It was found that BVW measured with Dean-Stark's method was consistently ranked with rock types, i.e., better rock types were associated with lower BVW, while poorer rock types were associated with higher BVW (Fig. 7b). Figure 8 shows the Buckles' plot constructed with core porosity and Dean-Stark water saturation, indicating a good correlation between rock types and BVW. The LPSA data from 24 core samples verify that grain size distribution and clay volumetric concentration are also closely related to hydraulic rock types (Fig. 9). In general, smaller median grain size indicates higher clay volumetric concentration and poorer hydraulic rock types. Figure 10 shows that MICP data are also ranked consistently with the defined rock types. Better rock types generally exhibit larger major pore throat sizes. Table 2 summarizes the statistical variability of total porosity, absolute permeability, and Dean-Stark water saturation together with BVW for each rock type.

Table 2: Statistical distributions of total porosity, absolute permeability, Dean-Stark water saturation and BVW, and volumetric clay concentration for each rock type in the offshore Trinidad field case.

	ϕ_t (frac)	k (mD)	Dean-Stark S_w (frac)	Dean-Stark BVW (frac)	C_{cl} (frac)
RT-1	0.231 ± 0.019	1255 ± 455	0.064 ± 0.036	0.014 ± 0.006	0.006 ± 0.003
RT-2	0.215 ± 0.014	358 ± 125	0.092 ± 0.019	0.020 ± 0.004	0.018 ± 0.005
RT-3	0.140 ± 0.023	52.5 ± 27.9	0.337 ± 0.105	0.045 ± 0.007	0.051 ± 0.018
RT-4	0.065 ± 0.016	3.2 ± 2	0.70 ± 0.22	0.056 ± 0.005	0.119 ± 0.027

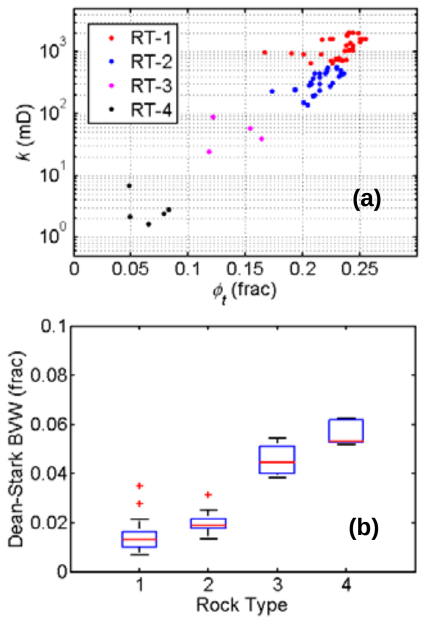

Fig. 7: (a) Porosity-permeability crossplot grouped according to rock types, and (b) box-plot of core-measured BVW grouped with rock types in the offshore Trinidad field case.

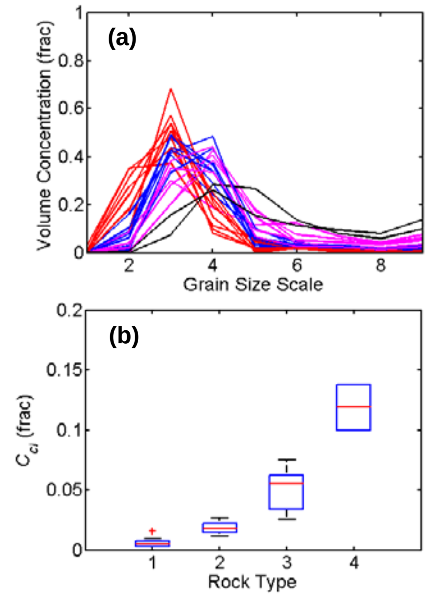

Fig. 9: (a) Grain size distribution data grouped according to rock types, and (b) box plot of clay volumetric concentration grouped according to rock types in the offshore Trinidad field case.

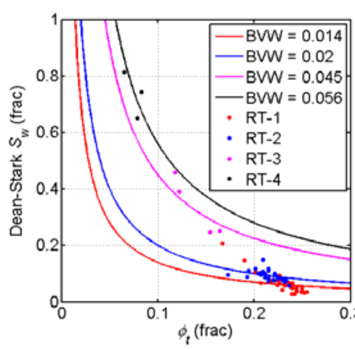

Fig. 8: Buckle's plot constructed with core porosity and Dean-Stark water saturation in the offshore Trinidad field case.

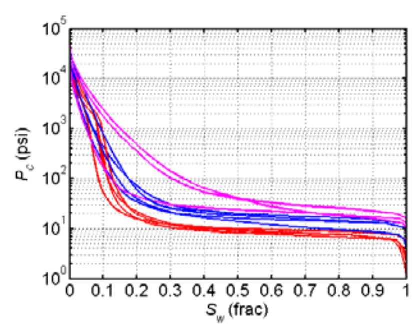

Fig. 10: MICP data color-coded with classified rock types in the offshore Trinidad field case. RT-4 was not studied by MICP.

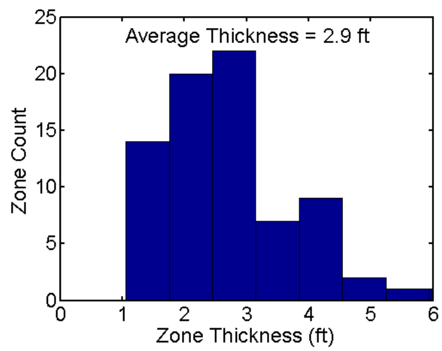

Fig. 11: Statistical distribution of petrophysical zone thickness in the Trinidad deltaic gas sand reservoir.

Petrophysical Zonation in CSF. The reservoir unit under analysis comprises a total depth interval of 260 ft; a scale that can be visually identified from seismic amplitude data. We use gamma ray, bulk density, and resistivity logs to segment the reservoir unit into 80 petrophysical zones with an average thickness of approximately 2.9 ft. Figure 11 shows the histogram of zone thickness. Most zones exhibit thicknesses ranging from 1.0 ft to 4 ft, which are mostly a mixture of more than one rock type.

Bayesian Rock Typing from Logs. After defining rock types and their associated petrophysical properties, we invoke Bayesian rock typing to infer the rock type distribution by iteratively testing hypothetical rock types. Figure 12, track 5, shows the final rock typing results: the vertical distribution of rock types with maximum likelihood and their associated uncertainty. Visual comparison indicates good agreement with core-derived rock types. It is also observed that, in general, thicker beds exhibit lower uncertainty.

Rock Types: Core vs. Well Logs. Table 3 shows a contingency table that compares rock types estimated via clustering of well logs to core-derived rock types; it indicates a low rate of agreement (in terms of the contingency coefficient, Bishop et al., 1975), roughly equal to 60%. Table 4 shows a similar contingency table comparing rock types estimated with the Bayesian method to core-derived rock types. In this case, the rate of agreement increases to 78%.

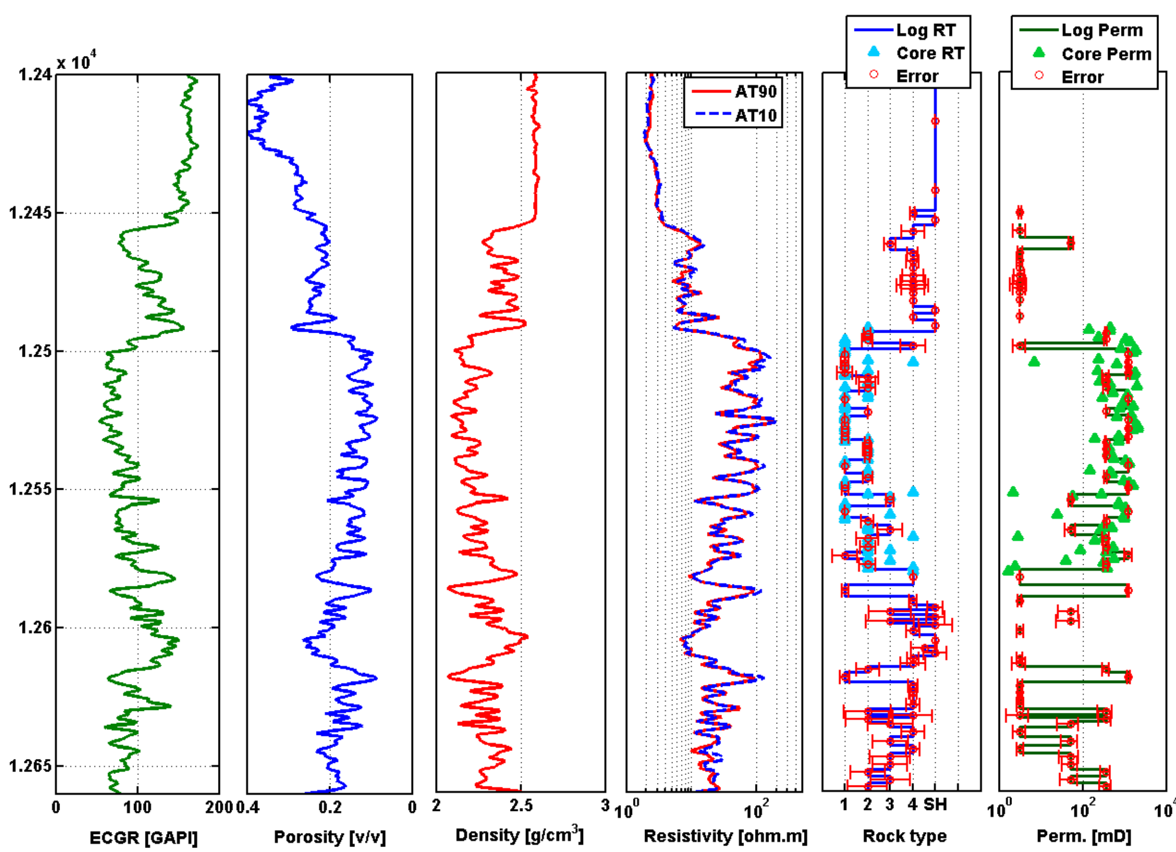

Fig. 12: Field case of Bayesian rock typing and uncertainty quantification. From left to right, Track 1: Gamma Ray; Track 2: Porosity; Track 3: Density; Track 4: Resistivity; Track 5: Rock type and uncertainty; Track 6: Permeability and uncertainty. Triangle marks in Tracks 5 and 7 identify core measurements.

Table 3: Contingency table of rock types determined with the conventional rock typing method in the offshore Trinidad field case. (Crammer's V = 0.44; Contingency Coefficient C = 60.7%).

Rock Type	1	2	3	4	Total
1	21	3	-	-	24
2	6	17	1	1	25
3	3	7	1	2	13
4	1	2	2	2	7
Total	31	29	4	5	69

Table 4: Contingency table of rock types determined with the Bayesian rock typing method in the offshore Trinidad field case. (Crammer's V = 0.71; Contingency Coefficient C = 77.7%).

Rock Type	1	2	3	4	Total
1	28	2	-	-	30
2	3	26	1	-	30
3	-	1	2	2	5
4	-		1	3	4
Total	31	29	4	5	69

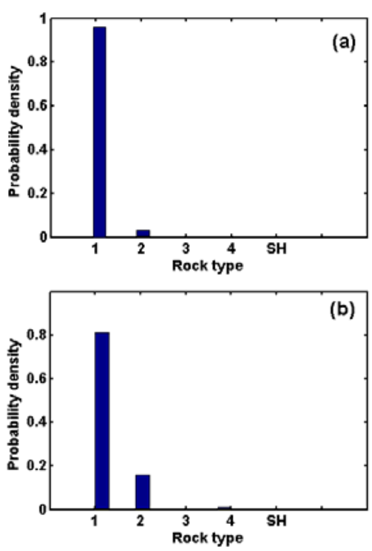

Fig. 13: Uncertainty of rock types quantified in two petrophysical zones in the offshore Trinidad field case. (a) thick bed at 12502 ft, and (b) thin bed at 12508 ft.

Uncertainty Analysis of Rock Types. Two sand layers of different thickness are selected to compare their associated rock-type uncertainties. Both layers are classified as rock type 1. Figure 13 shows that their uncertainties are quite different because of bed thickness, where the thicker bed centered at 12,502 ft exhibits relatively lower uncertainty.

Table 4 also shows that, in general, good rock types are less prone to misclassification. This behavior is partly due to the large population of good rock types, and partly due to their larger bed thickness. Xu et al (2012c) investigated the correlation between reservoir quality and bed thickness.

Permeability Estimation and Uncertainty Analysis. Each inferred distribution of rock types generates a corresponding permeability distribution obtained by calculating the permeability with rock-type specific porosity-permeability relations established with core data. A statistical analysis of all permeability distributions quantifies the uncertainty of permeability in each layer. Track 6 in Fig. 12 shows the distribution of maximum-likelihood permeability and its associated uncertainty. We observe that low rock-type uncertainty gives rise to low permeability uncertainty. Figure 14 shows the correlations between log-estimated permeability and core permeability. The correlation coefficient is improved from 0.62 with conventional rock typing method to 0.78 with the Bayesian estimation method (which explicitly corrects for should-bed effects on well logs).

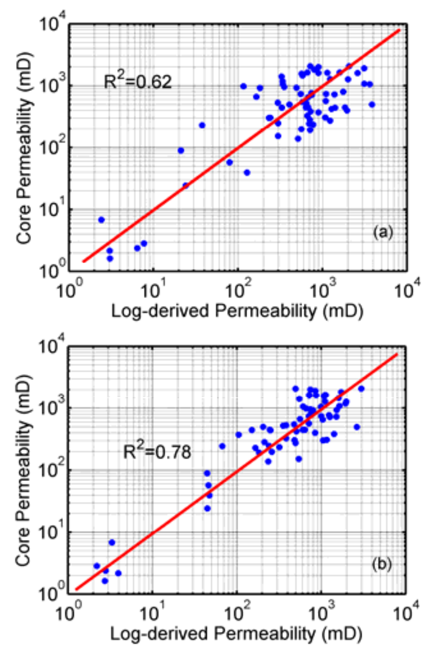

Fig. 14: Comparison of permeability estimation with (a) conventional rock typing method, and (b) Bayesian rock typing method in the offshore Trinidad field case.

Applications to Geological Interpretation. It is important to associate petrophysical rock types to depositional facies in reservoir description. Bed thickness and grain size are two important geological attributes that connect petrophysical rock types with depositional facies. In the field case, a clear correlation was established between petrophysical rock types and grain sizes. Therefore, a stack of vertical rock types provides useful information to geologists for interpretation of geological facies and to reduce uncertainty when constructing a stratigraphic reservoir model based on well logs.

Figure 15 compares the vertical distribution of rock types inferred in this paper against the sedimentological description performed with core measurements. The distribution of rock types is consistent with the geological framework and indicates an aggradational delta front with three facies in a coarsening upward trend: distal delta front interbedded with channelized slope turbidites and slump sheets, mouthbar facies interbedded with wave/storm- dominated proximal delta front facies, and proximal delta front facies (Bowman, 2002). In addition, the distribution of petrophysical rock types and the estimated permeability values provide additional details to construct a stratigraphic reservoir model for fluid flow simulation.

Computational Performance Analysis. A common disadvantage of stochastic estimation methods is the need to perform a multitude of forward calculations to sample the posterior probability function in model space. Yang and Torres-Verdín (2013) introduced two strategies to enhance the efficiency of the stochastic method, which reduce the CPU time to approximately 4 hours to obtain 100 realizations of hypothetical distributions of rock types (100 ft interval) on a desktop PC (3.4 GHz CPU) and Matlab platform. The computer time required by the calculations can be further reduced with the implementation of parallel-computing techniques.

CONCLUSIONS

We developed a new core-calibrated and log-based Bayesian rock typing method that employs fast numerical simulation of well logs for iterative hypothesis testing. The new method effectively reduces shoulder-bed effects on well logs which give rise to significant uncertainty in rock typing across thinly bedded formations. A probabilistic method was introduced and successfully verified for describing hybrid rock classes.

The application of the new method to a field case indicated more than 77% agreement between log- and core-derived rock types. Overall, the correlation between predicted permeability and core-measured permeability was improved by approximately 16% compared to conventional deterministic methods. In addition, the method quantified the uncertainty associated with rock-type identification and permeability estimation. The final distribution of maximum-likelihood rock types was consistent with the geological framework and provided useful information for stratigraphic reservoir construction and modeling.

Computational performance can be a limitation when implementing the Bayesian rock typing method in field studies because of the requirement of heavy data processing. However, the method remains accurate and

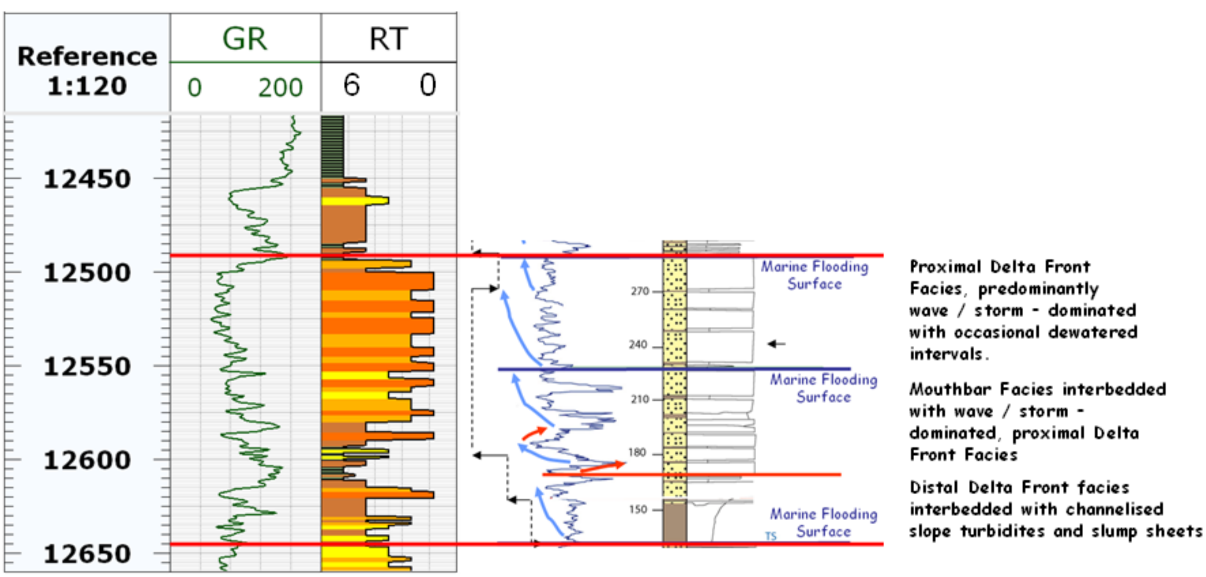

Fig. 15: Comparison between estimated rock types and core-based facies description. Left panel: rock types inferred with the Bayesian method; Right panel: facies description (Bowman, 2004).

reliable for detailed reservoir description in deepwater field developments where only a limited number of wells are available.

NOMENCLATURE

C : Contingency coefficient, ()
C_{cl} : Volumetric concentration of clay, (frac)
C_i : Volumetric concentration of mineral i, (frac)
$\mathbf{d}$: Vector of observed well logs, ()
$\mathbf{G}(\bullet)$: Forward function, ()
I_{max} : Maximal iteration number
L : Number of rock layers, ()
$\mathbf{m}$: Vector of rock type distribution, ()
N : Number of rock samples, ()
$p(\mathbf{m})$: A-priori distribution of model parameters, ()
$p(\mathbf{d}|\mathbf{m})$: Conditional probability distribution, ()
$q(\mathbf{m}|\mathbf{d})$: Posterior probability distribution for model parameters, ()
S_w : Connate water saturation, (frac)
V : Cramer's V, ()
ϕ_N : Neutron porosity, (frac)
ϕ_t : Total porosity, (frac)
σ_t : Apparent conductivity, (mS/m)
ρ_b : Bulk density, (gm/cm^3)
γ : Gamma ray, (gAPI)
χ^2 : Pearson's chi-squared test, ()

ACRONYMS

2D : Two Dimensional
BVW : Bulk Volume of Water
CPU : Central Processing Unit
HAFWL: Height Above Free Water Level
LPSA : Laser Particle Size Analyzer
MICP : Mercury Injection Capillary Pressure
SOBM : Synthetic Oil-Base Mud

ACKNOWLEDGEMENTS

We would like to thank BP Trinidad-Tobago (BPTT) for providing the field data used in this study. The work reported in this paper was funded by The University of Texas at Austin's Research Consortium on Formation Evaluation, jointly sponsored by Afren, Anadarko, Apache, Aramco, Baker-Hughes, BG, BHP Billiton, BP, Chevron, China Oilfield Services, LTD., ConocoPhillips, ENI, ExxonMobil, Halliburton, Hess, Maersk, Marathon Oil Corporation, Mexican Institute for Petroleum, Nexen, ONGC, OXY, Petrobras, Repsol, RWE, Schlumberger, Shell, Statoil, Total, Weatherford, Wintershall and Woodside Petroleum Limited.

REFERENCES

Archie, G.E., 1950, Introduction to Petrophysics of Reservoir Rocks, *AAPG Bulletin*, Vol. 34, No. 5, P. 943-961.

Archie, G.E., 1952, Classification of Carbonate Reservoir Rocks and Petrophysical Considerations, *AAPG Bulletin*, Vol. 36, No. 2, P. 278-298.

Aster, R. C., Borchers, B., and Thurber, C. H., 2005, *Parameter Estimation and Inverse Problems*, Elsevier Academic.

Bishop, Y. M. M., Fienberg, S. E., and Holland, P. W., 1975, *Discrete Multivariate Analysis: Theory and Practice*, MIT Press.

Bowman, A.P., 2004, Sequence Stratigraphy and Reservoir Characterization in the Columbus Basin, Trinidad, Ph.D. Dissertation, Imperial College London.

Buckles, R.S., 1965, Correlating and Averaging Connate Water Saturation Data, *Journal of Canadian Petroleum Technology*, Vol. 9, No. 1, P.42-52.

Geweke, J., 1991, Evaluating the Accuracy of Sampling-Based Approaches to the Calculation of Posterior Moments: Federal Reserve Bank of Minneapolis, Research Department Staff Report 148.

Ijasan, B., 2010, Rapid Modeling of LWD Nuclear Measurements Acquired in High-Angle and Horizontal Wells for Improved Petrophysical and Geometrical Interpretation, M.S. Thesis, The University of Texas at Austin.

John, A.K., Lake, L.W., Torres-Verdín, C., and Srinivasan, S., 2008, Seismic Facies Identification and Classification Using Simple Statistics, *SPE Reservoir Evaluation & Engineering*, Vol. 11, No. 6, P.984-990.

Leverett, M.C., 1941, Capillary Behaviour in Porous Solids, *Transactions of the AIME*, 142, P.159-172.

Liu, Z., Torres-Verdín, C., Wang, G. L., Mendoza, A., Zhu, P., and Terry, R., 2007, Joint Inversion of Density and Resistivity Logs for the Improved Petrophysical Assessment of Thinly-Bedded Clastic Rock Formations: Paper VV, *SPWLA 48th Annual Logging Symposium*, Austin, Texas, June 3-6.

Malik, M., Salazar, J. M., Torres-Verdín, C., Wang, G. L., Lee, H. J., and Sepehrnoori, K., 2008, Effects of Petrophysical Properties on Array-Induction Measurements Acquired in the Presence of Oil-Base Mud-Filtrate Invasion, *Petrophysics*, vol. 49, no. 1, pp. 74-92.

Mendoza, A., Torres-Verdín, C., and Preeg, W. E., 2010, Linear Iterative Refinement Method for the Rapid Simulation of Borehole Nuclear Measurements, Part I: Vertical wells, *Geophysics*, vol. 75, no. 1, pp. E9-E29.

Pittman, E.D., 1992, Relationship of Porosity and Permeability to Various Parameters Derived from Mercury Injection-Capillary Pressure Curves for

Sandstone, *AAPG Bulletin*, Vol. 76, No. 2, P. 191-198.

Voss, B., Torres-Verdín, C., Gandhi, A., Alabi, G., and Lemkecher, M., 2009, Common Stratigraphic Framework to Simulate Well Logs and to Cross-Validate Static and Dynamic Petrophysical Interpretations, *SPWLA 50th Annual Logging Symposium*, The Woodlands, Texas, USA, June 21-24.

Vrubel, N. K., 2007, Statistical Partitioning of Well Logs and Core Measurements to Detect and Quantify Petrophysical Properties, M.S. Thesis, The University of Texas at Austin.

Wang, G. L., Torres-Verdín, C., Salazar, J. M., and Voss, B., 2009, Fast 2D inversion of Large Borehole EM Induction Data Sets with an Efficient Fréchet-derivative Approximation, *Geophysics*, Vol. 74, no. 1, pp. E75-E91.

Xu, C., and Torres-Verdín, C., 2012, Saturation-Height and Invasion Consistent Hydraulic Rock Typing Using Multi-Well Conventional Log Data, *SPWLA 53rd Annual Logging Symposium*, Cartagena, Columbia, June 16-20.

Xu, C., Heidari, Z., and Torres-Verdín, C., 2012a, Rock Classification in Carbonate Reservoirs Based on Static and Dynamic Petrophysical Properties Estimated from Conventional Well Logs, *SPE Annual Technical Conference and Exhibition*, San Antonio, Texas, October 5-9.

Xu, C., Torres-Verdín, C., Ma, J., and Li, W., 2012b, Fluid Substitution Analysis to Correct Borehole Geophysical Measurements Acquired in Gas-Bearing Formations Invaded by Oil-Base Mud, *83rd SEG Annual Meeting*, Las Vegas, Nevada, USA, Nov 4-9.

Xu, C., Torres-Verdín, C., and Steel. R.J., 2012c, Facies Interpretation Based on Quantitative Analysis of Grain Size and Bed Thickness from Well Logs in Deepwater Turbidite Reservoirs, *AAPG Annual Convention and Exhibition*, Long Beach, LA, April 22-25.

Xu, C., and Torres-Verdín, C., 2013a, Rock-Type Based Analysis of Hydration Water Effect on Capillary Pressure in Shaly Sand Formations: a Case Study in a Deltaic Gas Reservoir, Offshore Trinidad, submitted to *Journal of Petroleum Science and Engineering*.

Xu, C., and Torres-Verdín, C., 2013b, Multi-Scale Orthogonal Rock Class Decomposition: Top-Down Reservoir Characterization Integrating Logs and Core in Tight Gas Sands, *54th SPWLA Annual Logging Symposium*, New Orleans, Louisiana, June 22-26.

Yang, Q., and Torres-Verdín, C., 2011, Efficient 2D Bayesian Inversion of Borehole Resistivity Measurements, *82nd SEG Annual Meeting*, San Antonio, Texas, USA, September 18-23.

Yang, Q., and Torres-Verdín, C., 2013, Joint Stochastic Interpretation of Conventional Well Logs Acquired in Hydrocarbon-Bearing Shale, *54th SPWLA Annual Logging Symposium*, New Orleans, Louisiana, June 22-26.

ABOUT THE AUTHORS

Chicheng Xu is currently a Ph.D. candidate studying integrated reservoir characterization through geologically and petrophysically consistent rock classification based mainly on well logs and core data. His research focuses on applying rock classification to fundamental reservoir characterization subjects such as permeability prediction, saturation-height modeling, uncertainty analysis, heterogeneity characterization, petrophysical upscaling, fluid substitution, and sedimentary facies interpretation. He had more than 10 technical papers published in SPWLA, SPE, SEG, SCA, and AAPG. He received his B.S. in Physics from the University of Science and Technology of China in 2002 and MPHIL in Physics from the Chinese University of Hong Kong in 2004. Before joining the Formation Evaluation Research Consortium group in the Department of Petroleum and Geosystems Engineering at the University of Texas at Austin, he worked at Schlumberger Beijing Geoscience Center as software engineer from 2004 to 2009.

Qinshan Yang is a research fellow with the Department of Petroleum and Geosystems Engineering at the University of Texas at Austin. He received a Ph.D. degree in Signal and Information Processing from the Chinese Academy of Sciences in 2003. His research interests include borehole geophysics, petrophysics, formation evaluation, well logging, integrated reservoir description, signal processing, and inverse problems. He has been working with the University of Texas at Austin since 2010. From 2006 to 2010, he worked as vice dean with the China National Petroleum Corporation Logging Research Institute. Before that, he worked for Schlumberger in BGC and IPC from 2003 to 2006.

Carlos Torres-Verdín received a Ph.D. in Engineering Geoscience from the University of California at Berkeley in 1991. During 1991–1997 he held the position of Research Scientist with Schlumberger-Doll Research. From 1997–1999, he was Reservoir Specialist and Technology Champion with YPF (Buenos Aires, Argentina). Since 1999, he has been with the Department of Petroleum and Geosystems Engineering of The University of Texas at Austin, where he currently holds the position of Zarrow Centennial Professor. He conducts research on borehole geophysics, formation evaluation, well logging, and integrated reservoir characterization. He is the founder and director of the Joint Industry Consortium on Formation Evaluation at the University of Texas at Austin.